SST Ensemble Experiment-Based Impact Assessment of Climate Change on Storm Surge Caused by Pseudo-Global Warming: Case Study of Typhoon Vera in 1959

SST Ensemble Experiment–Based Impact Assessment of Climate Change on Storm Surge Caused by Pseudo–Global Warming: Case Study of Typhoon Vera in 1959

Junichi NINOMIYA 1, Nobuhito MORI 2, Tetsuya TAKEMI 3, Osamu ARAKAWA 4

1 Faculty of Environmental Design, Kanazawa University

Kakuma-machi, Kanazawa, Ishikawa, 920-1192, Japan

jnino@se.kanazawa-u.ac.jp

2 Disaster Prevention Research Institute, Kyoto University

Gokasho, Uji, Kyoto, 611-0011, Japan

mori@oceanwave.jp

3 Disaster Prevention Research Institute, Kyoto University

Gokasho, Uji, Kyoto, 611-0011, Japan

takemi@storm.dpri.kyoto-u.ac.jp

3 Faculty of Life and Environmental Sciences, University of Tsukuba and Meteorological Research Institute

1-1-1 Tennodai, Tsukuba, Ibaraki, 305-8577, Japan

arakawa.osamu.ft@u.tsukuba.ac.jp

Abstract (200 words)

To evaluate future changes in storm surge caused by global warming, dynamical downscaling using the Weather Research and Forecasting model was conducted for Typhoon Vera under present- and future-climate conditions and storm surge simulation using the Coupled Model of Surge, Wave and Tide. The present-climate experiment entailed dynamical downscaling using data from the Japanese 55-year Reanalysis project as the initial and boundary conditions, and the future-climate experiments entailed downscaling considering future changes simulated through sea-surface temperature ensemble experiments using the Meteorological Research Institute Atmosphere General Circulation model. The characteristics of the downscaled typhoon agreed well with the Best Track, and the future changes in the typhoon characteristics were as follows: intensification of the central pressure, delayed decline in the high-latitude area, and westward track migration. Present-climate storm surge simulation executed using these downscaling results after correcting for the track error agreed with the observed surge, but the storm surges under future-climate conditions were underestimated because of differences in the typhoon track and surface roughness. Storm surge simulations were conducted using an empirical typhoon model; the results suggest a storm surge of 26 cm (average of the ensemble) at Nagoya Port, which is located in the innermost region of Ise Bay.

Keywords: climate change, storm surge, tropical cyclones, downscaling

1. Introduction

Numerous studies have investigated the environmental changes induced by global warming. For example, the risk of storm surges along coastal regions is expected to increase because of changes in the characteristics of tropical cyclones (TCs), but this phenomenon has not been adequately and quantitatively discussed at the regional scale. The fifth assessment report (AR5) of the Intergovernmental Panel on Climate Change (IPCC) reported that the number of TCs is expected to decrease but that their strength, maximum wind speed, and rainfall is likely to increase [IPCC-AR5, 2013]. TCs affect wide regions, particularity the tropical to the midlatitude regions. Intense TCs tend to induce storm surges, which in turn cause extensive damages; recent examples of this include Hurricane Katrina in 2005, Cyclone Nargis in 2008, Hurricane Sandy in 2012, Typhoon Haiyan in 2013, and Cyclone Winston in 2016. The probability of occurrence of storm surges is very low, but when they do occur, they substantially and adversely affect coastal regions. For example, Hurricane Katrina caused US$108 billion worth of economic losses, and Typhoon Haiyan caused 6,000 causalities.

Given the long-term nature of facility planning along coasts, high-certainty estimations are required for disaster reduction along coastal areas. Thus, future changes in storm surge characteristics must be considered in such estimations. The risk of storm surge is estimated by considering the possible maximum surge and the surge caused by future strong

typhoons. Future storm surge projections have been performed in several countries in Europe and East Asia. For example, Lowe and Gregory [2005] and Woth [2005] have analyzed future storm surges around the UK and in the North Sea regions, and they predicted significant increases in storm surge elevations, because of increased intensities of midlatitude storms, along the UK coast and the continental North Sea coast. Yasuda *et al.* [2014] estimated future storm surges by using the 5-km atmospheric model and reported shortened storm surge return periods. Yoshino *et al.* [2014] estimated future changes in the characteristics of possible maximum strength typhoons at Ise Bay, and Shibutani *et al.* [2015] discussed changes in the track of Typhoon Vera (1959) caused by possible maximum storm surges.

The climate change assessment of storm surges is important, but studies on future changes in storm surges as well as their long-term assessment in present-climate conditions are scarce, primarily because of the low probability (O(100) years) of and sensitivity of TC tracks to storm surge height at specific locations. Furthermore, storm surge projections are hindered by the lack of knowledge on changes to TC characteristics in these regions. Hence, long-term assessments of the TC risk at a particular region are difficult even under present-climate conditions alone. One method to overcome the drawbacks caused by the low occurrence of actual TCs is to use statistical modeling, and another method is to conduct pseudo–global warming (PGW) experiments by using a regional climate model (i.e., dynamical modeling)

[Mori and Takemi, 2016]. Dynamical model is a physically rational approach; however, establishing future-climate conditions for the dynamical model and controlling the typhoon characteristics (e.g., tracks) for storm surge modeling are difficult. For more information, the partial modification of initial and boundary condition in dynamical model as future-climate causes the loss of physically balance, for example, between air temperature and sea-surface temperature (SST), which influence heat flux. On the other hand, the overall modification may generate completely different typhoon as the storm surge event, and it makes comparison of storm surge difficult. The difference of the landfall location, even if typhoon has same characteristics, makes quite different storm surge.

This study examines future changes in storm surges by using PGW experiments in which several uncertainties of global and regional climate modeling are considered. PGW experiments were conducted for Typhoon Vera through SST ensemble experiments by using the 20-km Meteorological Research Institute Atmosphere General Circulation Model MRI-AGCM3.2S [Mizuta *et al.*, 2012]. Then, a series of PGW experiments is conducted for estimating future changes in atmospheric parameters, such as air temperature and pressure, using which future changes in typhoon characteristics are estimated. Uncertainties in the projections are discussed on the basis of the future SST distribution in space as obtained using the SST ensemble experiments. Finally, storm surge simulation using the future typhoon

intensity with same track is carried out, and the future changes of storm surge at Nagoya Port are evaluated.

2. Methodology

2.1 Outline of methodology

Future-climate conditions are projected using the general circulation model (GCM), which has been used in several studies on future TC characteristics. These studies were based on coarse-resolution GCMs (i.e., spatial resolution larger than 1°) such as MIROC5 [Watanabe *et al.*, 2010], HadGEM2 [The HadGEM2 Development Team, 2011]; however, understanding TC behavior by using coarse-resolution GCMs is difficult. Recently, higher-resolution GCMs (spatial resolution finer than 20 km) have been developed, and their outputs can be directly used for estimating future changes in typhoon characteristics. Storm surge is more local event and its simulation needs fine-resolution atmospheric information (i.e., spatial resolution smaller than a few kilometers).

Dynamical downscaling under present- and future-climate conditions using latest 20-km GCM output was performed to make the detail forcing for storm surge simulation. Subsequently, a series of storm surge simulations were executed. The Weather Research and

Forecasting (WRF) model [Skamarock *et al.*, 2008] was used for atmospheric modeling. The WRF model is used extensively by researchers because of the ease of preprocessing (e.g., making grids and establishing initial and boundary conditions) in this model. The Coupled Model of Surge, Wave and Tide (SuWAT; [Kim *et al.*, 2008]) was used for storm surge modeling. SuWAT couples the storm surge calculated using nonlinear shallow-water equations and the wind waves calculated using the spectral wave model SWAN [Booij *et al.*, 2001]; however, to reduce computational cost in this study, the wave model was not used, and the flooding, run-up, and inflow from the river were not considered. Thus, in this study, storm surge was simulated using the standard dynamical modeling approach.

Outline of this research is that present- and future-atmospheric forcing under TC event is downscaled by WRF using 20-km GCM, and storm surge simulations with downscaled forcing are carried out. Then, the future change of storm surge is examined. Characteristic aspects of this research are to check sensitivity for downscaling on future change parameters, to consider representative distribution pattern of future change to decrease uncertainty and to use dynamical downscaled forcing for storm surge simulation.

2.2 ***Dynamical downscaling of Typhoon Vera***

The present-climate (“Pre”) experiment was conducted using WRF and data from the

Japanese 55-year Reanalysis (JRA-55; Kobayashi *et al.*, 2015) project. JRA-55 provides data on three-dimensional atmospheric variables measured at a horizontal resolution of 1.25°. Accuracy of simulation for Typhoon Vera was verified by Ninomiya *et al.* [2015], and its reproducibility for intensity and track of typhoon is enough to use in this paper. Therefore, we used Typhoon Vera hindcast obtained using WRF and the JRA-55 as the baseline for storm surge modeling at Ise Bay. Table 1 lists the conditions used in WRF modeling, including nudging, typhoon bogus, and nesting. Two-domain nesting was applied to increase the accuracy of the hindcast of the eye structure and the related minimum central pressure. An accurate hindcast needs fine horizontal resolution on the order of a few kilometers. The extensive coarse domain and Kain–Fritsch scheme were used to resolve typhoon development, and the two-way nesting was used to account for the topographical characteristics of Ise Bay and its surroundings (Fig. 1). Furthermore, because surface wind strongly influences the storm surge hindcast, 56 fine-resolution vertical layers were set near the surface. Data from domain 2 must be cautiously used: The downscaling results in domain 2 yield more detail typhoon information, but the tracks under PGW conditions differed from the original track of Typhoon Vera. Hence, the results of domain 2 were not used for storm surge modeling because the typhoon tracks shifted westward.

Table 1

Fig. 1

The PGW experiments were dynamical downscaling by using data from the JRA-55 project and the global climate projections obtained through SST ensemble experiments by using

the 20-km MRI-AGCM3.2S model [Mizuta *et al.*, 2014]. These SST ensemble experiments were conducted as a 25-year time-slice experiment by using four future-change SST patterns from the Coupled Model Intercomparison Phase 5 (CMIP5) model under the Representative Concentration Pathways (RCP) 8.5 scenario as the bottom boundary condition of the AGCM. For a given bottom boundary in the AGCM, the SST ensemble experiments were conducted for four spatial patterns under future-climate conditions (Fig. 2, top panels).

Fig. 2

Future-climate conditions can be implemented in several ways. A simple method is to consider only the SST for downscaling in the PGW experiments. However, atmospheric stability strongly influences TC downscaling [Ito *et al.*, 2016]. The method to consider only SST will strengthen atmospheric instability, and sensitivities of future change parameters are need to examined to avoid unnatural instability. Therefore, various combinations of the SST, air temperature (T), and air pressure (P) can be examined to determine their effect on TC downscaling in future-climate conditions. The MRI-AGCM3.2S–based ensemble experiments were conducted for four SSTs (cases C0 to C3). C0 is based on ensemble-averaged SST of AOGCMs (Atmosphere-Ocean General Circulation Model) in the CMIP5 data set [Mizuta *et al*., 2014]. C1–C3 are based on three SSTs in future-change patterns obtained through the cluster analysis of the CMIP5 data set and were used to complement the historical climate conditions in the JRA-55 data set. The SST distributions of future change in C0-C3 in Northern North Pacific

have largest SST warming. Especially, C1 shows smaller warming pattern, and C3 shows larger warming pattern in Western North Pacific. Spatial averages of SST in C0-C3 are 3.26 K, 3.09 K, 3.23 K and 3.55 K, respectively. Future changes in humidity and wind fields were not considered because future changes in humidity are negligible, whereas winds substantially affect the typhoon tracks. Difference of the track will cause completely different storm surge. Thus, future change of wind wasn't considered in this research. Fig. 2 shows the future changes in surface temperature, near-surface air temperature, and sea-level air pressure around Japan; to clearly delineate the spatial patterns, future changes in cases C1–C3 are depicted as anomalies from those in C0. These future changes are added to the JRA-55 data set and used as the initial and boundary conditions in WRF downscaling. To examine the dependence of future-change parameters on TC climatology, PGW experiments were conducted under the following three combinations of parameters: SST (Case C0 SST), SST and T (Case C0 SST/T) and SST, T, and P (Case C0 SST/T/P). Table 2 lists the Pre and PGW experiments and the corresponding minimum central pressure of the typhoons. The results are examined later.

Table 2

2.3 ***Storm surge modeling***

To estimate future changes in storm surge induced by global warming, a series of storm surge simulations was executed using nonlinear shallow-water equations (i.e., the SuWAT model),

Table 3

Fig. 3

with the pressure and winds obtained from the Pre and PGW experiments in WRF modelling as forcing. Table 3 presents the conditions used in storm surge modeling, and Fig. 3 shows the domains used in the modeling, which are as similar to those in Shibutani *et al.* [2015]. Three-domain nesting was conducted from a resolution of 7290 m to 810 m. The nesting was two-way but wave induced surge was not considered in this study. The total computational period was 54 hours, including 6 hours of spin-up.

The observed and estimated storm surge heights at Nagoya port (denoted by * in domain 3) were compared. In this study, the results of dynamical downscaling were used directly, which induces small surge because the typhoon tracks significantly influence storm surges; for example, the tracks were shifted westward in the PGW experiments (explained in Section 3). Therefore, the pressure and wind fields were forced to the storm surge model by using three methods: A) original dynamical downscaling, B) dynamical downscaling shifted eastward to fit the typhoon center to the Best Track, and C) empirical typhoon modeling on the Best Track whose strength is obtained from dynamical downscaling at the same latitude. In the empirical typhoon model, Myers formula and the Fujii–Mitsuta formula [Fujii and Mitsuta, 1986] were used for pressure and wind, respectively.

3 Results and Discussion

3.1 ***Future changes in typhoon characteristics under pseudo–global warming conditions***

First, the results of the PGW experiments were analyzed to understand the dynamic properties of typhoons under future-climate conditions. The objective of the numerical setup of the WRF coarse domain was to resolve the typhoon development process by comparing the time series of several typhoon characteristics. The main target of the analysis was to validate the hindcast (Pre), the analysis of future changes, and sensitivity to climatological parameters.

Fig. 4 depicts the central pressure, maximum wind speed, and radius of maximum wind in the Pre and PGW experiments and the Best Track. The result of the Pre experiment shows good agreement with the Best Track although Typhoon Vera has the sharp development and low minimum pressure which are known as difficult phenomena for dynamical modeling. All PGW experiments estimated stronger typhoons than did the Pre experiments. The central pressure of the typhoon developed to 859.7 hPa in case C0 SST, which estimated large intensity changes in the typhoon relative to historical data because considering only SST reinforces atmospheric instability. Cases C0 SST/T and C0 SST/T/P estimated 889.4 and 893.0 hPa typhoons. All cases estimated a lower central pressure compared with the Pre experiment. Future changes in air pressure did not significantly affect minimum central pressure. The differences between C0 SST/T and SST/T/P become evident after landfall (9/26 12:00), and future changes in P gives were predicted to yield a stronger typhoon after landfall. Typhoon

Fig. 4

pressure under future-climate conditions considering P keeps strength after landfall comparing to C0 SST/T. The strong typhoons in the mid- to high-latitude regions can potentially induce large storm surges at vulnerable coasts (e.g., Seto Inland Sea and the Sea of Japan). Under future-climate conditions, the maximum wind speed correlated monotonically with the central pressure (Fig. 5), whereas future changes in the radius of maximum winds fluctuated largely, with no clear dependency. The results show that PGW experiment considering only SST estimates excessively strong typhoon that we have never experienced but future change including T restrained development of typhoon.

Fig. 5

Typhoon tracks are critical for impact assessment of storm surges; therefore, changes in typhoon tracks due to future changes warrants examination. Fig. 6 shows the typhoon tracks in the Pre and PGW experiments. The Pre experiment track agrees well with the Best Track, but the typhoon translation speed of the Pre track was slower than that of the Best Track. The tracks in the PGW experiments shifted westward by 100–150 km from the Best Track, which is consistent with the results in a similar PGW experiment by Ito *et al* [2016] and Kitoh *et al.* [2016] on other typhoons. Fig. 7 presents the central pressure, maximum wind speed, and radius of maximum wind under Pre and four PGW conditions. The typhoon strength in the Pre experiment agreed with the Best Track above 22 N. The difference in the minimum central pressure in the Pre and PGW experiments was approximately 9 hPa, and the typhoon track

Fig. 6

Fig. 7

moved westward by nearly 2°. Future changes in peak intensity were small (9 hPa), but all PGW experiments estimated strong typhoons of 20 hPa at latitudes above 25 N. Similarly, future changes in maximum wind speed was estimated to be larger by approximately 10 m/s at latitudes above 25 N. At 33–35 N, the difference in typhoon intensities in the Pre and PGW experiments was small because the shift in the typhoon track varies with the landfall latitude.

These results indicate that the risk of storm surge along the coast of Japan would increase in the future. Although the radius of maximum wind did not significantly change under the future conditions, future typhoon tracks are expected to shift westward. The changing future spatial SST patterns in the SST ensemble experiments demonstrate that the minimum pressure change is approximately 9 hPa in the four investigated future SST patterns.

The local distributions of pressure and wind around the storm surge assessment area are important because the maximum storm surge height can be considered the sum total of pressure- and wind-induced surges. Figs. 8 and 9 show the spatial distribution of minimum pressure at mean sea level and that of maximum wind speed, respectively. The pressure distributions clarify that typhoon intensity weakens at landfall. The Pre typhoon became weaker from latitude 30 N onward, but the PGW typhoons retained their strength up to just before landfall. The typhoons in the PGW experiments exhibited lower central pressure than those in the Pre experiments. However, the Pre typhoon had a larger impact on the storm surge at Ise

Fig. 8,9

Bay than did the PGW typhoons; this is primarily due to the differences in the typhoon tracks. The maximum wind speed is distributed to the right side of the track, and in the Pre experiment, Ise Bay is located on the right side. Accordingly, severe storm surge will be simulated in Ise Bay under Pre condition which has the distribution of high wind speed and low pressure around Ise Bay. However, the peak maximum wind speed in C0 and C3 under future-climate conditions occurred around Osaka Bay (150 km west of Ise Bay). The peak maximum wind speeds (~30 m/s) in C1 and C2 occurred at Kinki district. Differences in the roughness of land and sea greatly affect the attenuation of wind speed. These differences are climatologically nonsignificant, but they are significant in storm surge assessment.

The future changes in typhoon pressure and wind, which majorly affect storm surge, were investigated through the PGW experiments. The future-climate condition in the PGW experiments strengthened the typhoon to approximately 9 hPa because of the 3.28 K increase in SST. However, in the PGW experiments, the case in which only SST changes were considered generated an unrealistically strong typhoon. The effect of future changes in pressure on the central pressure of typhoons is relative small, but these changes result in typhoon intensity being high only at higher latitudes. All PGW experiments generated stronger typhoons whose tracks generally shift westward relative to the Best Track. The distributions of minimum pressure and maximum wind speeds are expected to significantly influence storm surge.

3.2 ***Storm surge hindcast***

Compared with the data observed under the present-climate condition, dynamical downscaling by using WRF yielded reasonable results for the typhoon track, pressure, and wind field. Storm surge hindcasts were generated using the abovementioned pressure and wind fields as well as the empirical typhoon model developed using observed parametric information. The empirical model was used to evaluate the storm surge distribution and to indirectly validate the pressure and wind distribution given by the WRF model. The distributions of maximum storm surge heights of Typhoon Vera were examined by implementing three atmospheric forcing conditions: (A) direct use of WRF dynamical downscaling (top panels in Fig. 10), (B) WRF dynamical downscaling with the track shifted to match the Best Track (middle panels in Fig. 10), and (C) the aforementioned empirical typhoon model (bottom panels in Fig. 10). According to the observed data, Typhoon Vera induced 3.45-m storm surges at Nagoya Port, which is located at the end of the western bay (Ise Bay). Forcing condition A clearly underestimated the surge near Nagoya Port (location (a)). Shibutani *et al.* (2015) pointed out that storm surge is very sensitive to typhoon track, and this result would show that the typhoon track of dynamical downscaling has the error on the order of several tens kilometers.

Fig. 10

Forcing condition B yielded reasonable surge predictions along the coast, except for

Table 4

locations at the end of the eastern bay (Mikawa Bay), which demonstrates that forcing condition B yields reasonable estimations in areas of maximum wind speed (Table 4). However, the overestimation at the innermost of Mikawa Bay indicates that dynamical downscaling at a resolution of 5 km could not adequately capture the eye structure, including the eye walls. Capturing the eye structure of the tropical cyclone needs grid spacing of 2 km or less [Gentry & Lackmann, 2009]. The surge heights obtained using forcing condition C agreed well with the actual observations at Nagoya Port; however, the surge heights at other locations were underestimated, and high surge is concentrated at Nagoya Port. Lack of a homogeneous structure of typhoon including marginal area would cause concentrated surge.

Dynamical downscaling underestimated the storm surge, although the Pre experiment track agreed well with the Best Track (Fig. 6). By contrast, the surge predicted by forcing condition B showed good agreement with the observations, which evidences the sensitivity of storm surge to typhoon track. The surge predicted by forcing condition C agreed well with the observations at the inner sections of Ise Bay but yielded underestimated surges at other locations. Thus, the empirical typhoon model is suitable for evaluating storm surge at the innermost area of Ise Bay ignoring the accurate reproducibility of the storm surge throughout the bay.

3.3 ***Future changes in storm surge***

Storm surge simulations with the forcing conditions B and C under the Pre experiment condition agreed well with the observed surge height at Nagoya Port. The storm surge simulations under the future-climate conditions were executed on the basis of the results of the PGW experiments. Fig. 11 presents the observed and simulated time series of storm surge at Nagoya Port under forcing in the Pre and PGW experiments in WRF domain 1. The result of the Pre experiment underestimated the surge because of the typhoon track deviated from the Best Track, and the time of peak surge was delayed because of the slow typhoon moving speed just prior to landfall. Fig. 10 and Table 4 shows the underestimation of storm surge height at inner location point in Ise Bay when using forcing condition A. The results of all PGW experiments underestimated the surge heights because the typhoon tracks shifted westward by more than 100 km from the Best Track. The track deviations were due to future change in SST/T/P, and no appropriate method is currently available to manipulate the typhoon track during dynamical downscaling. Therefore, future change of wind which affects typhoon track is eliminated in dynamical downscaling, and track shifted forcing is used for storm surge simulation.

Fig. 11

The observed and calculated time series of surge heights at Nagoya Port in the Pre and PGW experiments when using east-shifted forcing are presented in Fig. 12. Although the spatial resolution of forcing is slightly coarse (5 km), the timing and height of the peak surge in the Pre experiment is in good agreement with the observed surge, which indicates that high

Fig. 12

effectiveness of the adjustment of the typhoon center in the particular case of small track error. The PGW experiments yielded smaller storm surge heights than did the Pre experiment. These smaller surges and the time lag of the peak were caused by changes in wind distribution around the typhoon eye, which in turn is due to deviation from the Best Track. Because the typhoon tracks in the PGW experiment were shifted more than 100 km westward, the relative positions from the Best Track to the Ise Bay migrated to the land; this resulted in a change of surface roughness, which in turn caused the underestimation surface winds. Small-scale data correction for the location is effective, but such corrections must be performed cautiously on a large scale.

Fig. 13

Fig. 13 shows the anomaly of the peak storm surge height and the corresponding time of occurrence for all computational conditions. The squares, triangles, and asterisks in Fig. 13 are cases of forcing conditions A, B, and C, respectively. An obvious error can be seen in the timing of the peak surge height when using forcing condition A under the present-climate condition. The anomaly of maximum storm surge height in forcing condition A was -2 to -0.5 m. Forcing condition C yielded the same time lag because the typhoon radius does not change much in the empirical model, whereas the central pressure and maximum wind speeds are considered to be major future changes. All PGW experiments estimated larger storm surge heights than the mean of the Pre experiment. According to the aforementioned results, the mean future change in storm surge at Nagoya Port was 26 cm.

A series of storm surge simulations with forcing conditions A to C were executed for the evaluation of future changes in storm surge at Ise Bay. The surge obtained when using forcing condition B under the present-climate condition agreed well with the observed result. However, surge estimated under the future-climate conditions were sensitive to the typhoon track. The surge estimated through empirical downscaling yields reasonable change without dependency of the distribution of pressure and wind around typhoon. According to RCP8.5 and the MRI-AGCM3.2H model, the storm surge is estimated to increase by 26 cm in the future.

Fig. 14 presents the ratio of changes in storm surge change obtained using PGW to SST changes in the Western North Pacific. SST changes represents the spatial average value related to typhoon intensification. Both dynamical downscaling and shifted downscaling do not have adequate accuracy to evaluate future changes in storm surge risk because of errors in the typhoon track and in the distribution of pressure and wind. Therefore, the PGW conditions yielded smaller storm surges than the presently observed storm surge. This result shows that the estimation of future changes in storm surge through a series of dynamical downscaling has large uncertainty. Future changes in storm surge were evaluated using the storm surge simulation and the empirical typhoon model. Ensemble average of maximum storm surge is 0.77 cm/K. According to the results of this study, changes in the storm surge risk in the future does not appear to be one of change in surge height but of change in the location of the surge.

Fig. 14

4 Conclusions

Dynamical downscaling experiments under present- and future-climate conditions were performed for Typhoon Vera. Future changes were obtained through SST ensemble experiments by using the MRI-AGCM3.2S model. Storm surge simulations were conducted under different forcing conditions of pressure and wind distribution, namely dynamical downscaling, forcing conditions B and C. The results of dynamical downscaling under the Pre condition showed that the estimated typhoon intensity and track agreed well with the Best Track, but a slight delay was observed in typhoon translation. However, the typhoon track was not adequately accurate for storm surge simulation. The results of PGW experiments conducted under different parameter combinations showed that the case in which only future changes in SST were considered yielded an unrealistically strong typhoon; considering future changes in T restrained this excessive typhoon development. The typhoon predicated after accounting for future changes in SST, T, and P weakened slowly. The typhoon tracks shifted westward in estimations obtained for all SST patterns.

Considering pressure and wind distribution eliminated the delay in typhoon movement under the Pre condition; thus, good estimations of storm surge could be obtained. However, simulating storm surges in PGW experiments through dynamical downscaling yields inaccurate

estimations because all typhoon tracks were shifted westward. Evidently, some methods, such as the method in which dynamical downscaling is combined with various initial condition using typhoon bogus, are effective in evaluating future storm surges due to strong typhoons [Oku *et al.*, 2014].

Acknowledgements

This work was conducted under JSPS KAKENHI and Integrated Research Program for Advancing Climate Models supported by the Ministry of Education, Culture, Sports, Science and Technology-Japan.

References

Booij, N., Holthuijsen, L. & Ris, R. [2001] "The "SWAN" wave model for shallow water," *Coast. Eng. Proc.*, **1**(25). doi:http://dx.doi.org/10.9753/icce.v25.

Fujii, T. & Mitsuta, Y. [1986] "Synthesis of a stochastic typhoon model and simulation of typhoon winds," *Disaster Prevention Research Institute Annals B* **29**, 229-239.

Gentry, M. S. & Lackmann, G. M. [2009] "Sensitivity of simulated tropical cyclone structure and intensity to horizontal resolution," Mon. Weather Review **138**: Issue 3, 688-704, doi:10.1175/2009MWR2976.1.

The HadGEM2 Development Team: Martin, G. M., *et al.* [2011] "The HadGEM2 family of met office unified model climate configurations," *Geosci. Model Dev.* **4**, 723-757, doi:10.5194/gmd-4-723-2011.

IPCC-AR5 [2013] "Climate Change 2013: The Physical Science Basis," (Cambridge Univ. Press).

Ito, R., Takemi, T. & Arakawa, O. [2016] "A possible reduction in the severity of typhoon wind in the northern part of Japan under global warming: a case study," *SOLA* **12**, 100-105.

Kim, S. Y., *et al.* [2015] "The role of sea surface drag in a coupled surge and wave model for Typhoon Haiyan 2013," *Ocean Modelling* **96**(1), 65-84.

Kitoh, A., et al. [2016] "Dynamical Downscaling for Climate Projection with High-Resolution MRI AGCM-RCM," *J. Met. Soc. Jpn Ser. II* **94A**, 1-16.

Kobayashi, S., *et al.* [2015] "The JRA-55 reanalysis: General specifications and basic characteristics," *J. Met. Soc. Jpn Ser. II* **93**(1), 5-48.

Lowe, J. A & Gregory, J. M [2005] "The effects of climate change on storm surges around the United Kingdom," *Phil. Trans. R. Soc. A* **363**, 1313-1328; DOI: 10.1098/rsta.2005.1570.

Mitsuyasu, H. & Honda, T. [1982] "Wind-induced growth of water waves," *J. Fluid Mech.* **123**, 425-442.

Mizuta, R., *et al.* [2012] "Climate simulations using MRI-AGCM3.2 with 20-km grid," *Met.*

Soc. Jpn **90A**, 233-258.

Mizuta, R., *et al.* [2014] "Classification of CMIP5 future climate responses by the tropical sea surface temperature changes," *SOLA* **10**, 167-171.

Mori, N. & Takemi, T. [2016] "Impact assessment of coastal hazards due to future changes of tropical cyclones in the North Pacific Ocean," *Weather & Climate Extremes* **11**, 53-69, doi: 10.1016/j.wace.2015.09.002.

Ninomiya, J., Takemi, T. & Mori, N. [2015] "Dynamical downscaling of Typhoon Vera for storm surge hindcast based on JRA-55," *J. JSCE Ser. B2 (Coast. Eng.)* **71**, 1699-1704.

Oku, Y., *et al.* [2014] "Assessment of heavy rainfall-induced disaster potential based on an ensemble simulation of Typhoon Talas (2011) with controlled track and intensity," Nat. *Hazards Earth Syst. Sci.* **14**, 2699-2709.

Skamarock, W. C., *et al.* [2008] "A description of the advanced research WRF version 3," **NCAR/TN-475+STR**, 125.

Shibutani, Y., *et al.* [2015] "Estimation of worst-class tropical cyclone and storm surge, and its return period -Case study for Ise Bay-," *J. JSCE Ser. B2 (Coast. Eng.)* **71**, 1513-1518.

Watanabe, M., *et al.* [2010] "Improved climate simulation by MIROC5: Mean states, variability, and climate sensitivity." *J. Climate* **23**, 6312-6335, doi: 10.1175/2010JCLI3679.1.

Woth, K. [2005] "North Sea storm surge statistics based on projections in a warmer climate:

How important are the driving GCM and the chosen emission scenario?" *Geophys. Res. Lett.* **32**, L22708, doi:10.1029/2005GL023762.

Yasuda, T., *et al.* [2013] "Projection for future change of storm surges around Japanese coasts using non-hydrostatic RCM outputs," *J. JSCE, Ser. B2 (Coast. Eng.)* **69**, 1261-1265.

Yoshino, J., Takashima, R. & Kobayashi, T. [2014] "A predicting technique of long-term variability of maximum potential storm surge heights considering future climate projections," *J. JSCE Ser. B2 (Coast. Eng.)* **70**, 1251-1255.

Table 1 Computational conditions used in WRF modeling.

Item	Setting (domain 1, 2)
Periods	1959/9/22 0:00 to 1959/9/27 0:00 (UTC)
Horizontal Resolution	5 km, 1 km
Horizontal Grids	976 × 831, 401 × 401
Vertical layers	56
Microphysics	WRF Single-Moment 6-class
Shortwave Radiation	RRTMG (Rapid Radiative Transfer Model for GCMs) shortwave
Longwave Radiation	RRTMG longwave
Surface Layer	Revised MM5 Monin-Obukhov
Planetary Boundary	YSU (Yonsei University) scheme
Land Surface	5-layer thermal diffusion
Cumulus	Kain–Fritsch
Topography, Landuse	USGS GTOPO30 (Global 30 Arc-Second Elevation)
Nudging	Spectral Nudging (wave number 2, domain 1 above 700 hPa)
Bogus	Initial condition on domain 1

Table 2 Pre and PGW experiments list and their minimum central pressure.

Case	Future-Change Parameter	Minimum Central Pressure [hPa]
Best Track	Not applicable	895
Pre	Not applicable	901.8
C0 SST	SST	859.7
C0 SST/T	SST, T	889.4
C0 (SST/T/P)	SST, T, P	893.0
C1	SST, T, P	894.7
C2	SST, T, P	891.3
C3	SST, T, P	891.2

Table 3 Computational conditions used in storm surge modeling.

Item	Setting (domain 1, 2, 3)
Periods	1959/9/24 18:00 to 1959/9/27 0:00 (UTC)
Horizontal Resolution	7290 m, 2430 m, 810 m
Grids	240 × 180, 228 × 213, 201 × 180
Tide	Not applicable
Drag Coefficient	Mitsuyasu and Honda [1982] (Constant for U10 > 30 m/s)

Table 4 Maximum storm surge at (a) in Fig. 8: Nagoya Port (upper value) and (b) in Fig. 8: innermost of Mikawa Bay (lower value), and observed surge were 3.45 m and 2.80 m, respectively (Unit: m).

Forcing	Pre	C0	C1	C2	C3
A	2.79 2.83	1.51 1.01	1.87 1.46	1.84 1.26	1.69 1.23
B	3.52 3.75	2.94 1.56	2.19 2.02	2.04 2.48	2.55 2.25
C	3.46 2.07	3.55 1.99	3.71 2.06	3.80 2.09	3.73 2.10

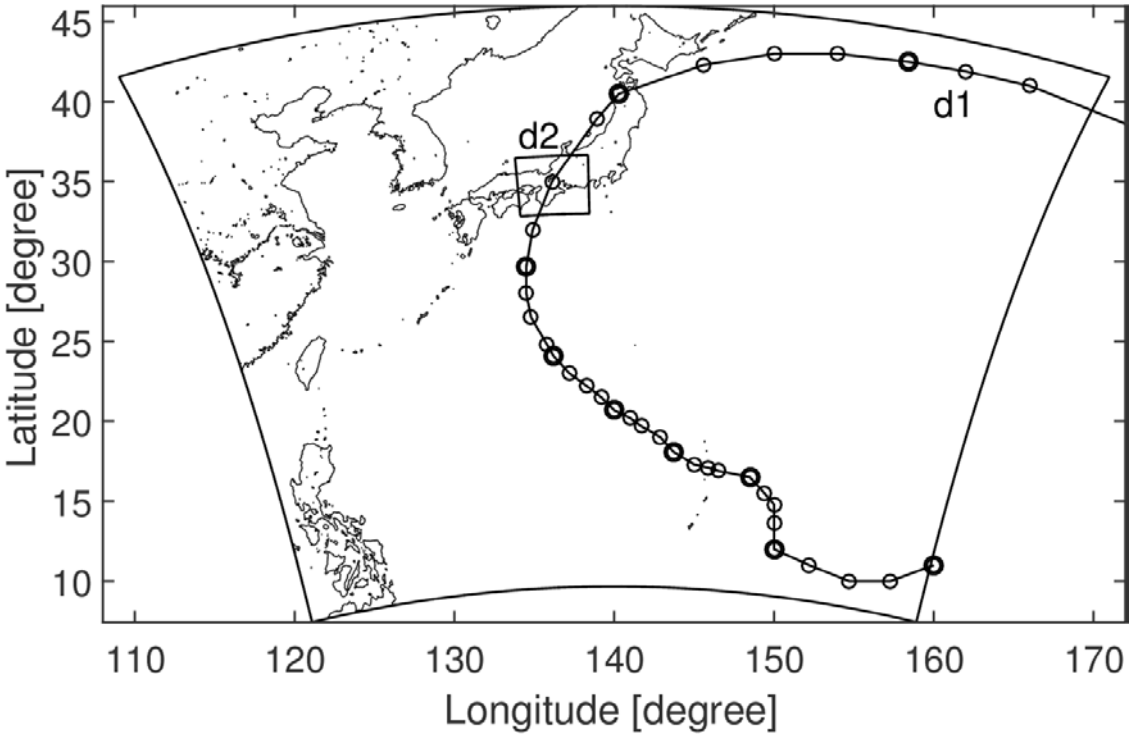

Fig. 1 Computational domain 1-2 used in typhoon modeling (WRF). Solid line and circles are typhoon track and locations at every 6 hours, respectively.

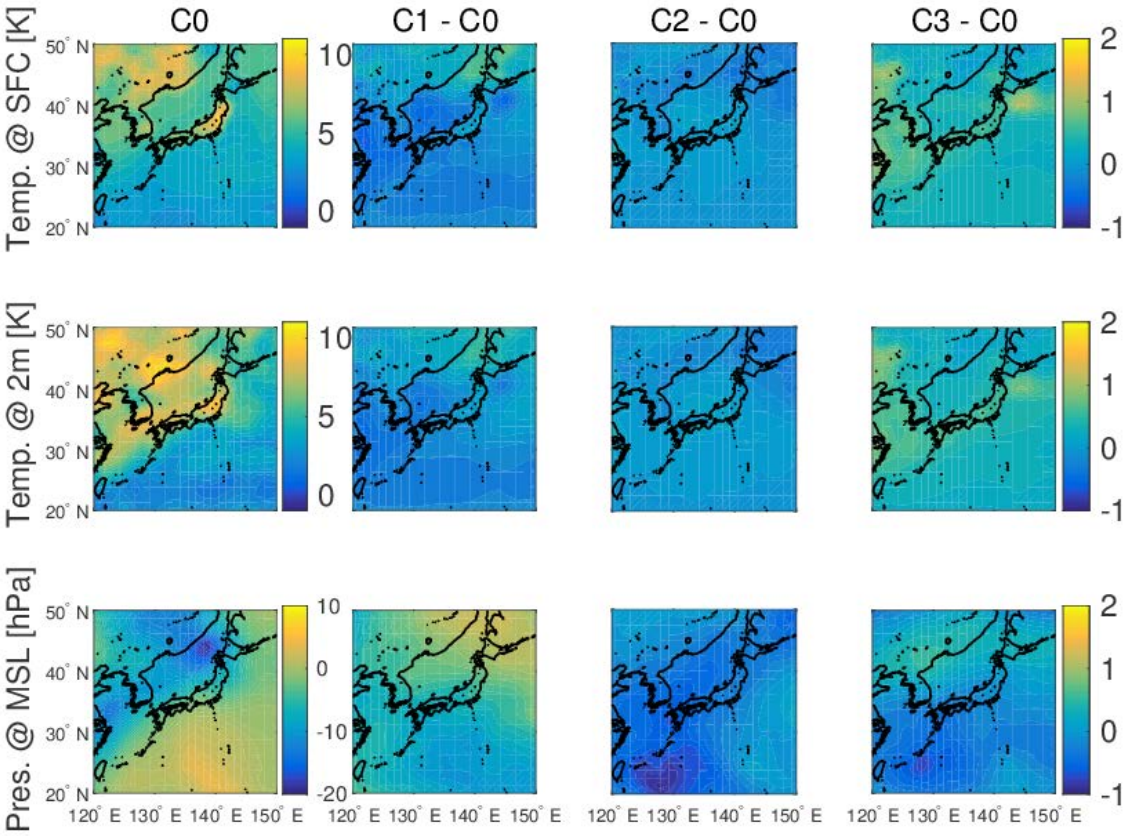

Fig. 2 In the SST ensemble experiments, future changes in surface temperature [K] (top row), in near-surface air temperature [K] (middle row), and the pressure at mean sea level [hPa] (bottom row) (left-most column: baseline condition C0; other columns: difference from C0).

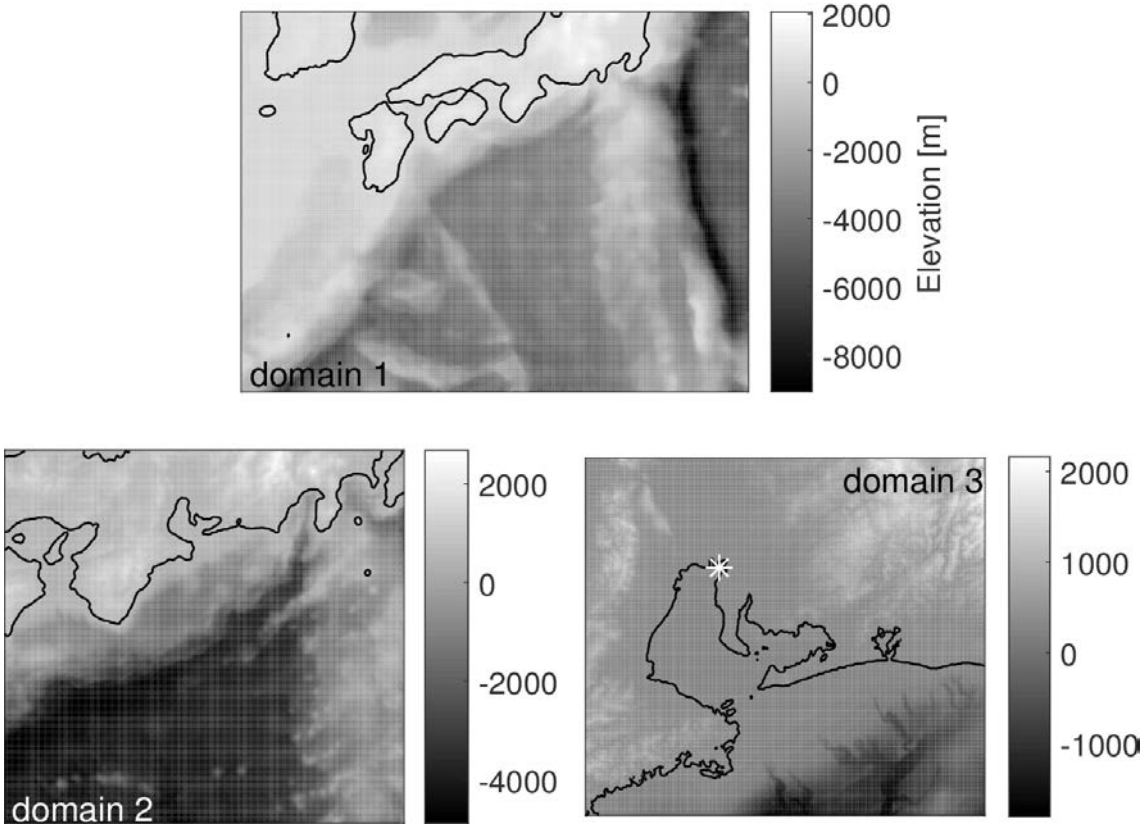

Fig. 3 Computational domains 1–3 used in storm surge modeling (* is Nagoya Port location).

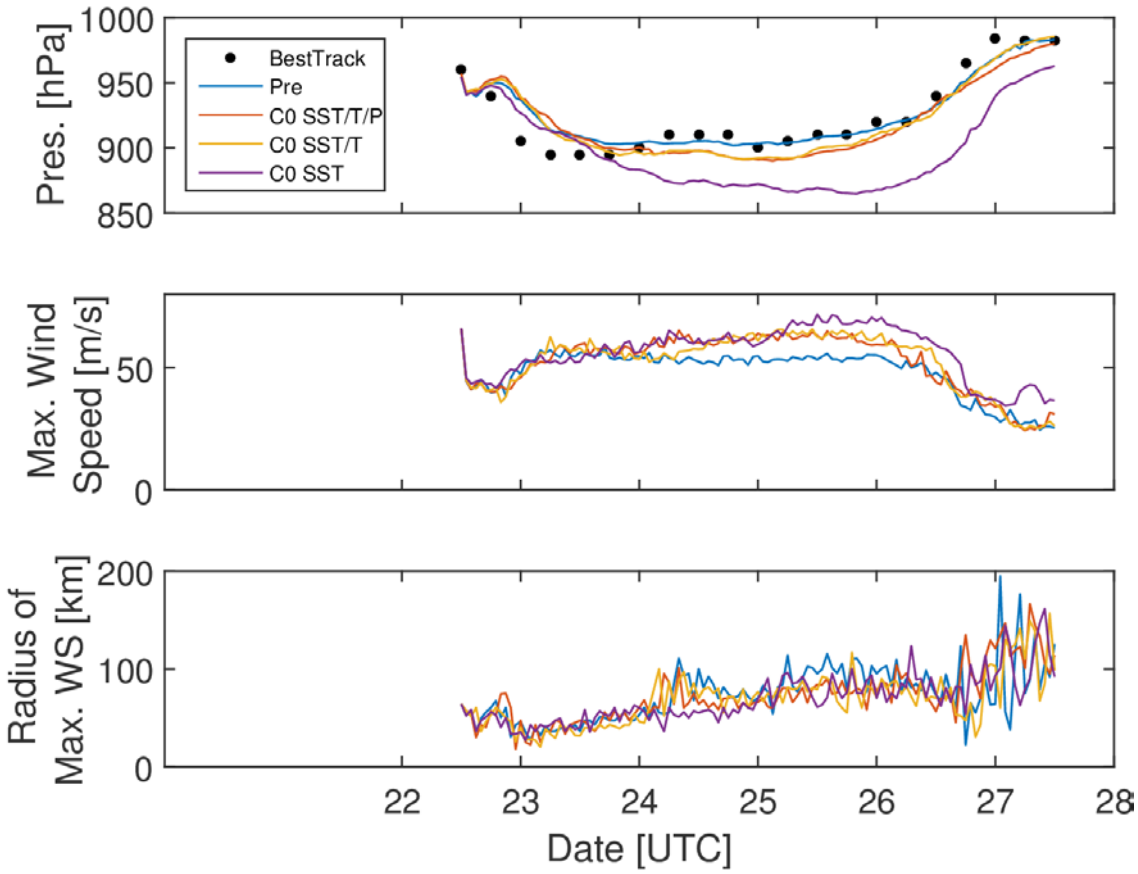

Fig. 4 Time series of the central pressure of typhoon, maximum wind speed, and radius of maximum wind for the Pre and PGW experiments and the Best Track.

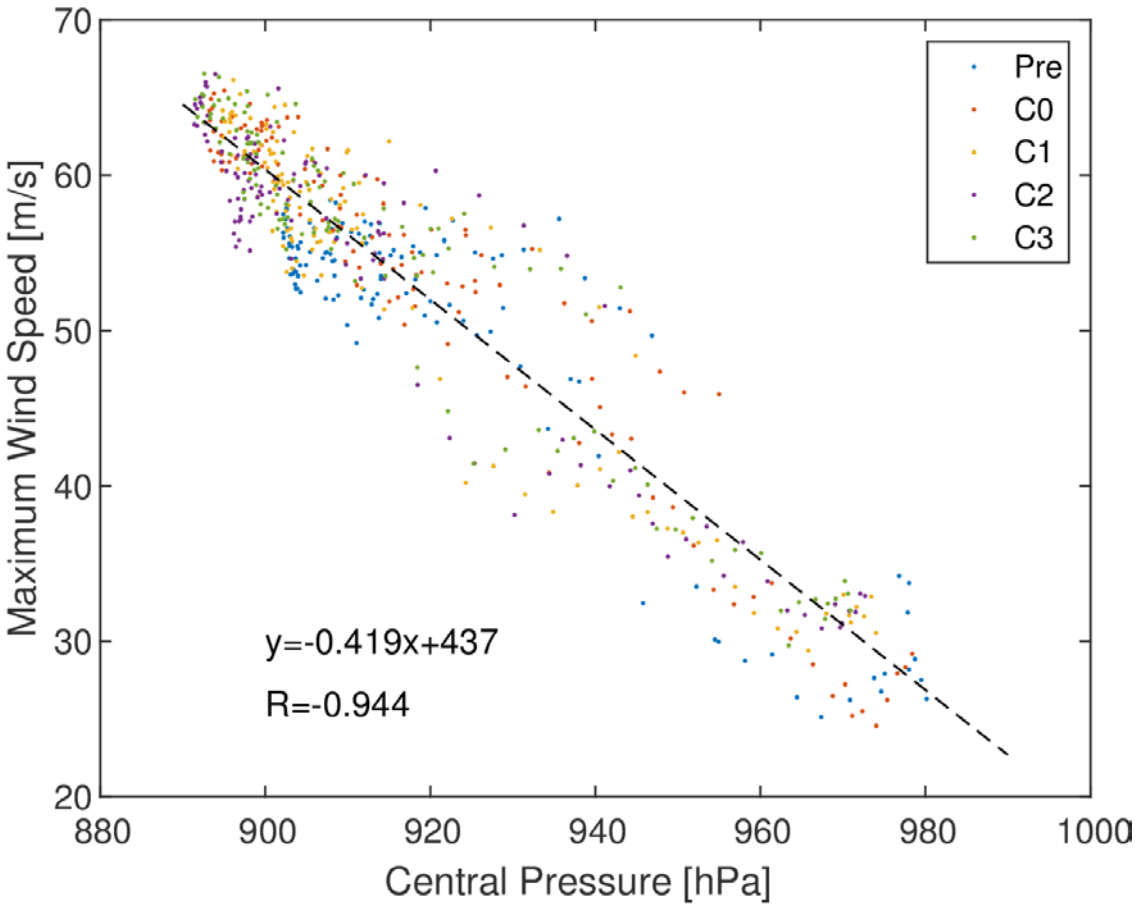

Fig. 5 Relationship between central pressure and maximum wind speed of typhoon.

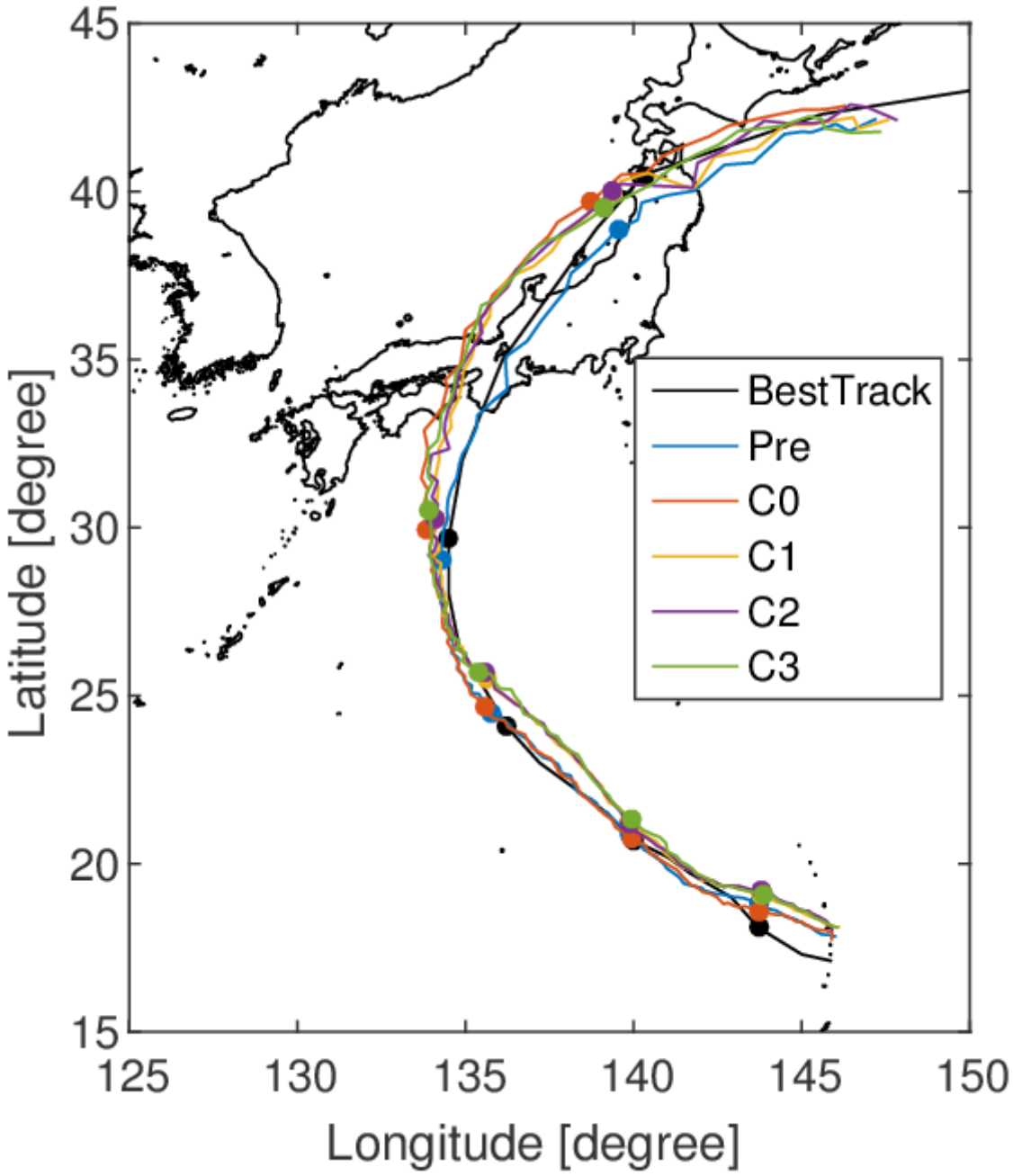

Fig. 6 Simulated typhoon tracks for the Pre and PGW experiments and the Best Track.

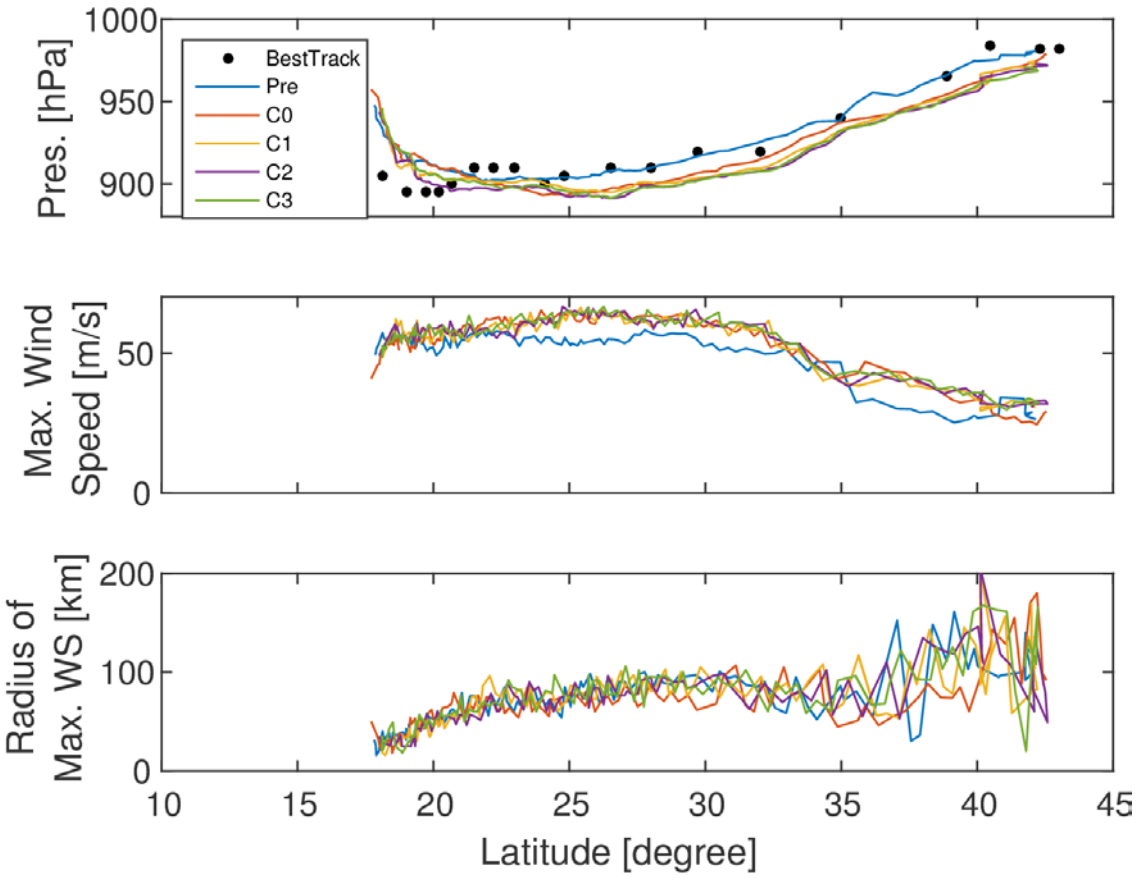

Fig. 7 Central pressure, maximum wind speed, and TC radius for the Pre and PGW experiments at various latitudes and the Best Track.

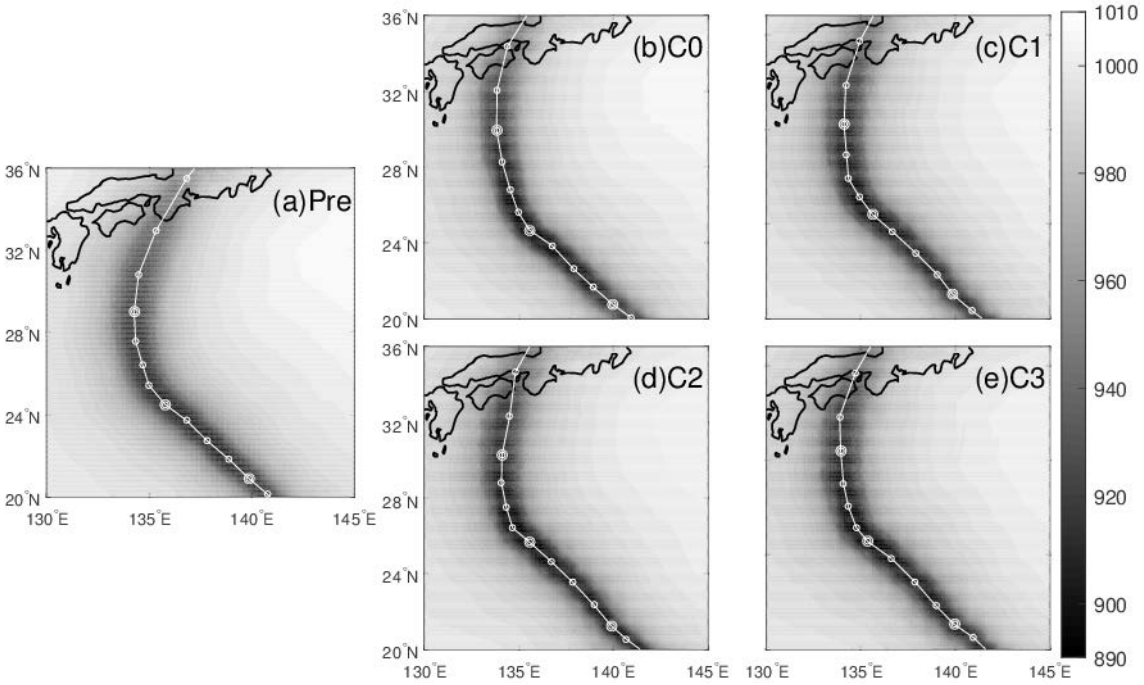

Fig. 8 Distribution of minimum pressure at mean sea level for the Pre and PGW experiments.

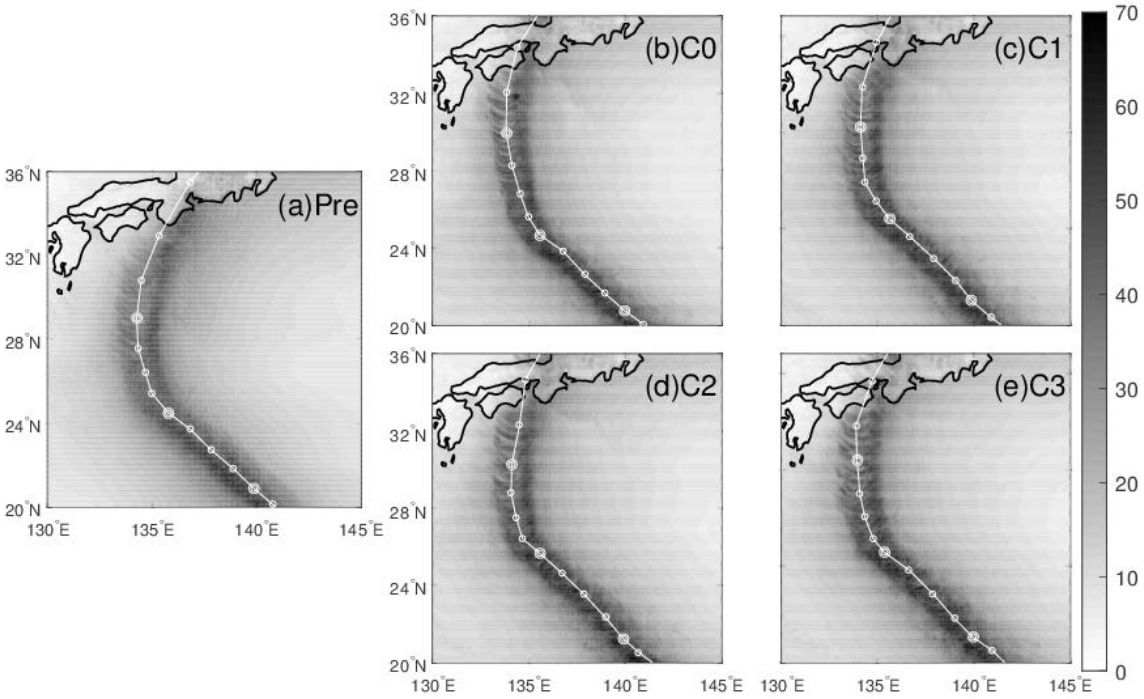

Fig. 9 Distribution of maximum wind speed at 10 m height for the Pre and PGW experiments.

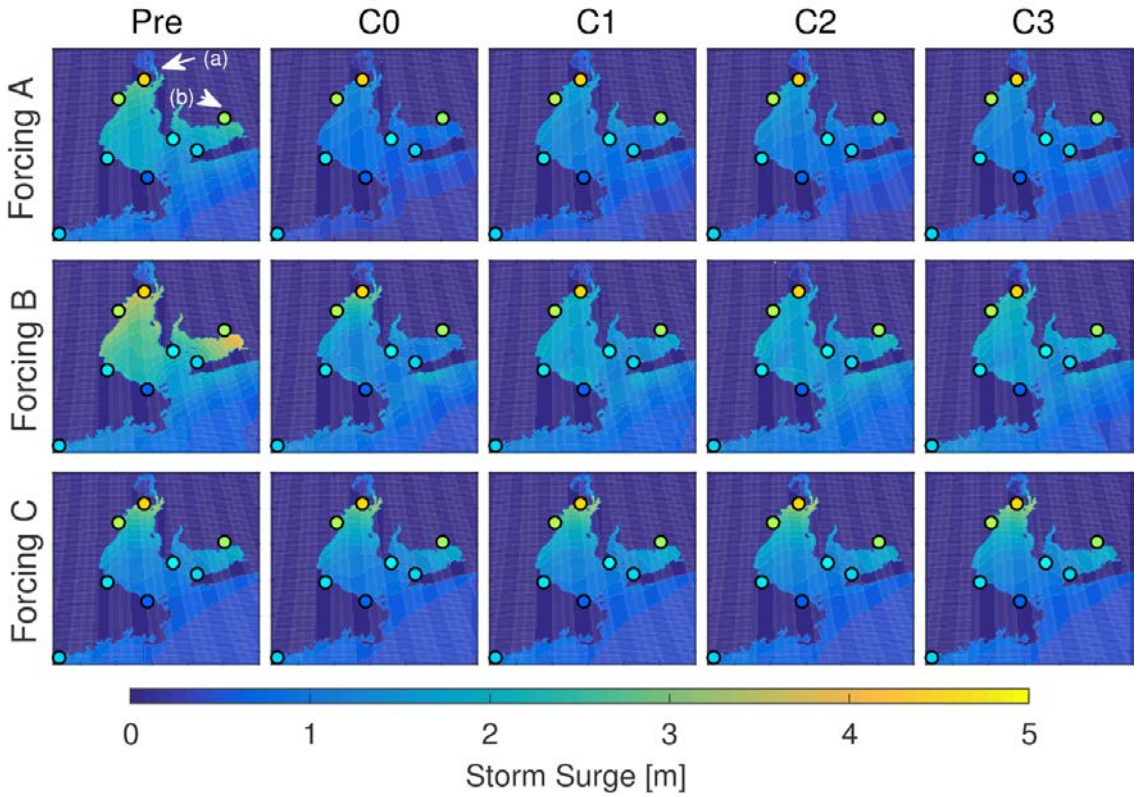

Fig. 10 Distributions of maximum storm surge height (top panels: forcing condition A; middle panels: forcing condition B; bottom panels: forcing condition C; columns (left to right): Pre, C0, C1, C2, and C3); color scale: the surge height in meters; circle: observed surge height at the locations; (a) and (b): locations of Nagoya Port and of innermost of Mikawa Bay corresponding to Table 4.

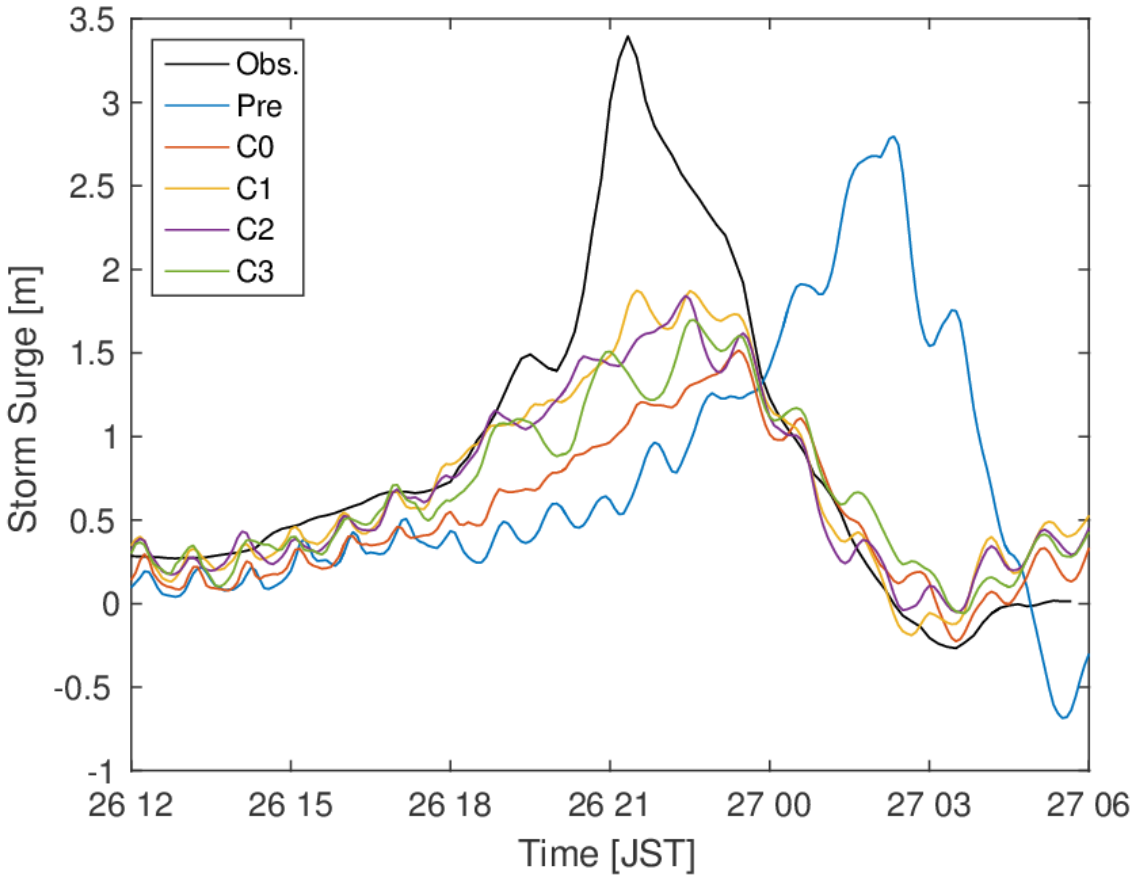

Fig. 11 Time series of storm surge height at Nagoya Port for the Pre and PGW experiments with forcing condition A as well as the observed surge height.

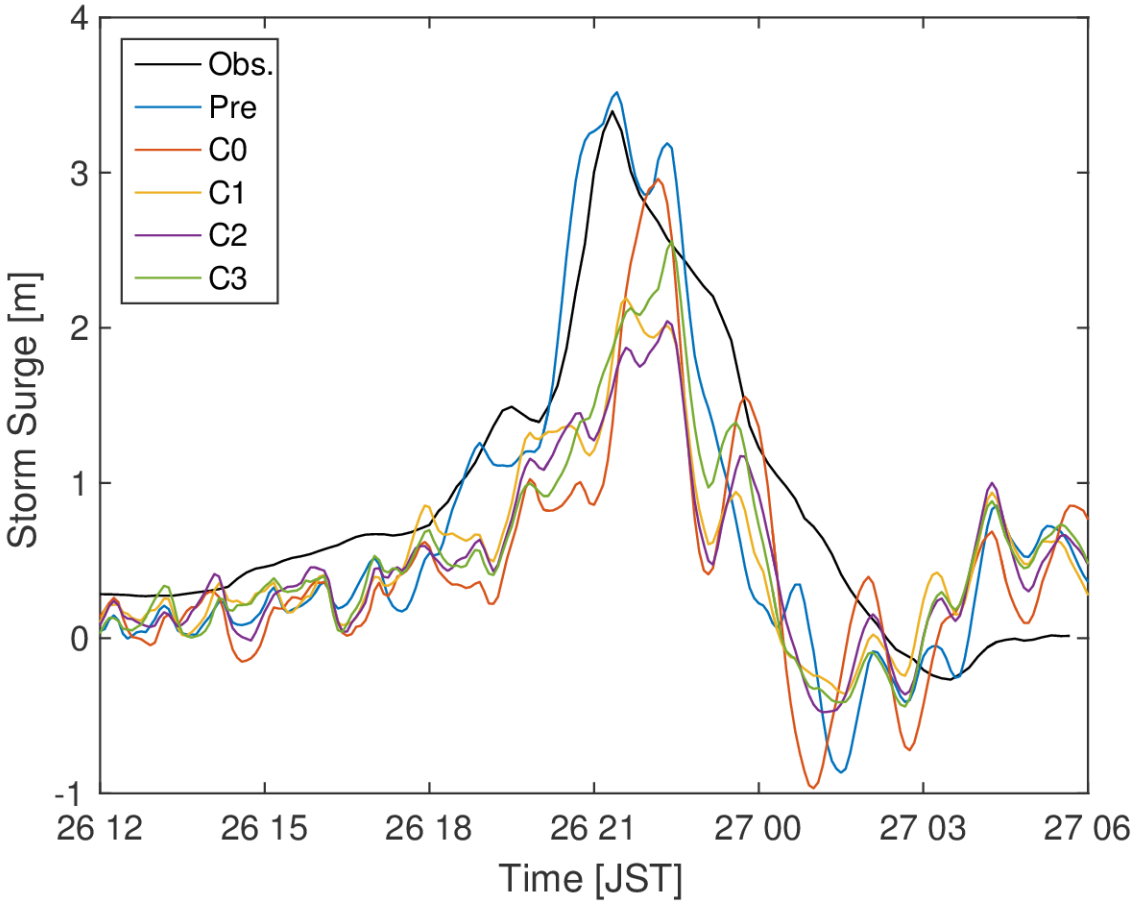

Fig. 12 Time series of storm surge height at Nagoya Port for the Pre and PGW experiments with forcing condition B as well as the observed surge height.

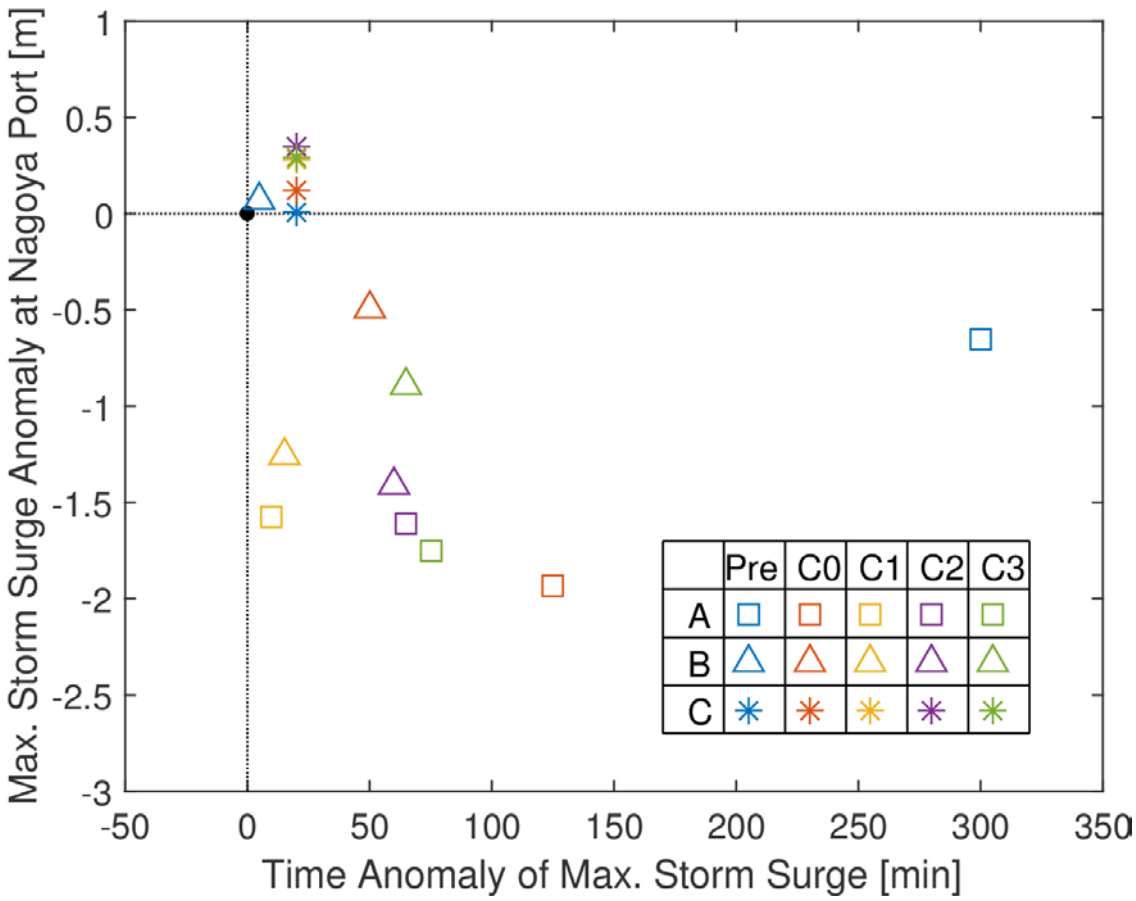

Fig. 13 Peak surge height (m) and its occurred time (min) in the Pre and PGW experiments and the observed surge height (square: forcing condition A, triangle: forcing condition B, asterisk: forcing condition C, blue: Pre, red: C0, yellow: C1, purple: C2, green: C3).

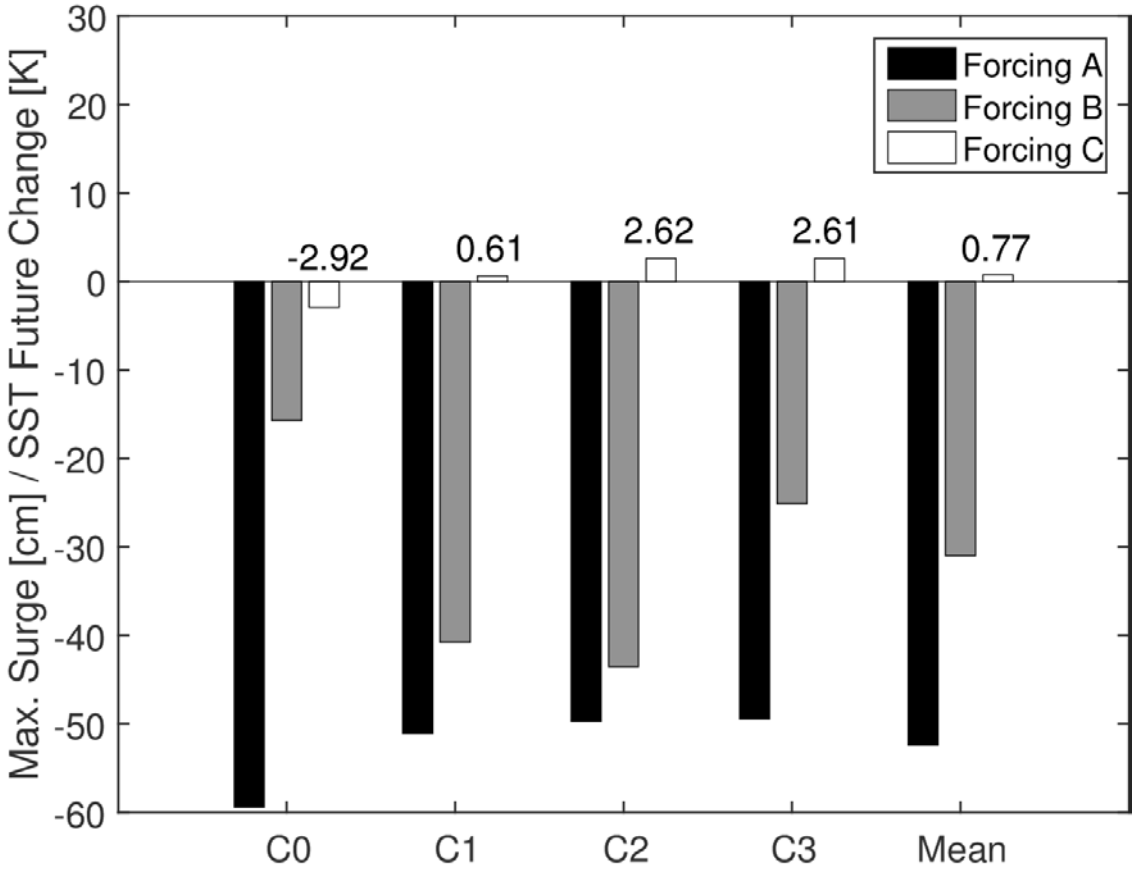

Fig. 14 The ratio of changes in storm surge due to PGW experiments to averaged SST in the Western North Pacific.